Journal of Manufacturing Processes 82 (2022) 777–791

Contents lists available at ScienceDirect

Journal of Manufacturing Processes

journal homepage: www.elsevier.com/locate/manpro

A novel current sensor indicator enabled WAFTR model for tool wear prediction under variable operating conditions

Pradeep Kundu [a,b], Xichun Luo [a,*], Yi Qin [a], Wenlong Chang [a], Anil Kumar [c]

[a] Centre for Precision Manufacturing, DMEM, University of Strathclyde, G1 1XJ, UK
[b] Center for Intelligent Maintenance Systems, University of Cincinnati, OH 45221, USA
[c] College of Mechanical and Electrical Engineering, Wenzhou University, 325035, China

ARTICLE INFO

Keywords:
Health indicator
WAFTR
Current sensor
Tool wear prediction
Machine learning

ABSTRACT

The health indicators (HIs) were extracted from the current sensor to represent the tool wear progression. The extracted HIs were found poorly correlated with the progression of tool wear as the raw current sensor signal was susceptible to the influence of other parts and structures in the machine tool. Hence, this paper proposed a novel current sensor-based HI that utilized the mean of inverse hyperbolic cosine function fitted to an envelope of the current signal to improve the correlation. Using the extracted HIs, many bespoke machine learning (ML) models have been developed by researchers. However, these models have many hyperparameters, difficult to interpret and especially poor prediction accuracy has been observed under variable operating conditions. This study overcame these issues by proposing a Weibull Accelerated Failure Time Regression (WAFTR) model, which combines process parameters data with HI for improving the prediction accuracy under variable operating conditions. This model mapped a functional relationship with tool wear in the form of probability density function to identify best HIs and acceleration/deacceleration factors which makes it interpretable. The acceleration/deacceleration factors are useful to deaccelerate the tool wear evolution by controlling the specific values of the machining parameters.

1. Introduction

The contact forces and friction between the cutting tool and workpiece during machining, high temperatures in the cutting area and chips pressure on the cutting tool will lead to gradual wear of the cutting tool or its sudden breakage [1,2]. Hence, a cutting tool condition monitoring system is needed to monitor tool degradation and timeliness detection of tool failure to improve productivity and product quality [3].

Cutting tool condition monitoring can be performed using direct or indirect methods [4,5]. The direct methods involve visual inspection of tool surfaces using optical instruments. However, direct methods are costly, time-consuming, and may interfere with machining operations. In indirect methods, tool condition is estimated based on the sensor signals such as vibration, acoustic emission, current, force, etc. [6–8]. The sensors used for condition monitoring, such as vibration, acoustic emission (AE), and force, may interfere with cutting operations, and measurements may also be affected by cutting fluid and cutting chips. In addition, separate mounting arrangements are also needed for the installation of these sensors. In comparison, current sensors can be mounted directly, e.g., Fluke i3000s to the machine tool's spindle external power supply connections and are cost-effective [5,9]. In some CNC machines, the current sensor is already installed and, hence, an integral part of the machine tool spindle. No separate arrangements are required for using the current sensor, and the measurement will not interfere with machining operations. Hence, the current sensor-based machine tool condition monitoring system is presented in this study.

The current signal is too complex to interpret directly. Hence a health indicator (HI) was often constructed to monitor tool wear degradation. The machine learning or statistical models can be used to mapped the relationship between extracted HIs and tool wear [10]. For example, Proteau et al. [11] presented a specific cutting energy HI to monitor the tool wear, which calculated the amount of energy required to remove 1 cm^3 of material. Utilizing the extracted HI, long short-term memory (LSTM) was used to tool wear prediction. Cai et al. [6] developed an LSTM model in which a temporal encoder was used to extract fault relevant HIs from the raw sensor signal time sequences. Later, these HIs were combined with process data and fed into a nonlinear regression model for tool wear prediction. Zhou and Sun [5] utilized the mean of

* Corresponding author.
E-mail address: xichun.luo@strath.ac.uk (X. Luo).

https://doi.org/10.1016/j.jmapro.2022.08.036
Received 22 December 2021; Received in revised form 4 March 2022; Accepted 10 August 2022
Available online 30 August 2022

signal amplitude in time-domain, frequency-domain and time-frequency domain to represent the progression of tool wear. These HIs are fed into a two-layer angle Kernel Extreme Machine Learning model (TEKELM) for online prediction of tool wear. The proposed TEKELM overcomes the shortcomings of KELM for preselecting the kernel function and its hyperparameter. Traini et al. [12] extracted various time-domain, frequency-domain and polynomial regression coefficients based HIs for tool wear monitoring. Among extracted HIs, best HIs were selected using a few criterions such as (a) removing HIs with low coefficient of variation, (b) removing the HIs with low correlation coefficients, (c) hypothesis testing and (d) removing HIs with low prognosability and monotonicity. Utilizing selected HIs, the neural network model was resulted in least error in prediction.

In the proposed studies discussed above, HIs were extracted based on the overall behaviour of the raw current signal (i.e., carrier signal). A poor correlation with tool wear progression was observed with these existing HIs. Hence, this study first focused on a signal processing strategy that can extract fault relevant hidden local information's from the raw current sensor signal, which is based on the signal envelope utilizing the Hilbert transform approach. An inverse hyperbolic cosine function was fitted to enveloped signal for sensitivity enhancement, and later the obtained signal was used for HI construction. Using the obtained HI, the existing machine learning (ML) models such as artificial neural network (ANN) [13,14], kernel extreme learning machine (KELM) [5,15], convolution neural network (CNN) [4,16], random forest regression (RFR) [12], recurrent neural network (RNN) [11], long short term memory (LSTM) [6,11,16,17], deep belief network [13], transfer learning [18,19], etc. can be used for tool wear prediction. However, these models work like a black box, don't have good interpretability (except RFR, which is partially interpretable), and the prediction errors are high under variable operating conditions. Few other interpretable statistical models such as Hidden Markov Model (HMM) [20,21], Kalman filtering [22], Particle filtering [23] can also be used for tool wear prediction. However, both Kalman filtering and Particle filtering approaches require an analytic form of state equations describing the physics of tool wear degradation which is complex and many times difficult to derive [24]. On the contrary, HMM is based on state transition probabilities learning from data but is impossible to use under variable operating conditions [24]. This study proposes a Weibull accelerated failure time regression (WAFTR) model for tool wear prediction to overcome the challenges of both statistical models and ML models. The proposed model will have inbuilt HI selection capability and is computationally faster compared to machine learning models such as KELM, CNN, RNN, LSTM, etc. The WAFTR model describes acceleration and deacceleration of wear as a function of HIs and operating conditions/process parameters and hence will be fully interpretable.

The raw sensor signal obtained for one cycle of machining may contain large fluctuations because the tool may not be in constant contact with the workpiece or have random reasons. The HIs extracted from this complete one cycle signal may not be able to map the tool wear evolution. No generic methodology is available to select the portion of the signal in which the actual machining process occurs, i.e., the tool is in constant contact with the workpiece. Therefore, a novel binary segmentation (BS) methodology is also proposed in this study to automatically filter the signal of interest and outlier removal. This methodology will identify the stationary phase of the machining activity in one cycle of operation.

In comparison to existing work on cutting tool wear prediction, the present study made the following attempts for an accurate and robust tool wear prediction:

- A novel HI based on the mean of inverse hyperbolic cosine function fitted to an envelope signal is proposed.
- A fully interpretable reliability-based WAFTR algorithm that can model both HIs and operating conditions simultaneously in a functional form with tool wear has been presented. The acceleration and deacceleration factor provided by this model is very important to control the tool wear evolution by changing the cutting tool parameters. No ML model provides acceleration and deacceleration factors to control the tool wear progression.
- A binary segmentation methodology has been proposed to remove the outliers and select the raw sensor signal that corresponds to the stable machining process.

This paper is divided into five sections. Section 2 discusses the overall tool wear prediction framework, the proposed data filtering and outlier removal methodology, current sensor based HIs for tool wear monitoring, and the WAFTR model for tool wear prediction. Section 3 describes the data sets used for validation of the proposed tool wear prediction framework. Comparison of tool wear prediction results obtained using the proposed methodology and existing methodologies are discussed in Section 4. The conclusion drawn based on the proposed work is presented in Section 5.

2. Proposed framework for tool wear prediction

This study proposes a unified and generic predictive tool condition monitoring framework that can be applied to different machining operations. The proposed framework for tool wear prediction combines data filtering and outlier methodology, health indicator (HI) extraction methodology, and wear prediction methodology. Fig. 1 shows the flow chart of the proposed framework for tool wear prediction.

The proposed framework is divided into two phases: offline and online. Current signal-based HIs correlating to tool wear progression will be extracted and identified in the offline phase. The process parameters such as depth of cut (DOC), feed rate, etc., will be combined with the current sensor-based extracted HIs for tool wear prediction under variable operating conditions. Based on the given tool wear data, corresponding process parameters, and current sensor HI values, machine learning or reliability-based models will be trained. The trained model performance will be checked based on performance metrics such as percentage error in prediction. The model parameters corresponding to which model gives the least prediction error will be obtained. In the online phase, using the raw current signal obtained for a new cutting tool, tool wear can be predicted based on the trained model and the most suitable HIs identified in the offline phase.

The novel data filtering and outlier removal, HI extraction, and tool wear prediction methodologies that are part of the proposed tool wear prediction framework are discussed hereunder.

2.1. Data filtering and outlier removal

The signal obtained from sensors may be unstable due to unexplained (e.g., random) and explained reasons such as the start and end of machining processes (e.g., the tool may not be in constant contact with the workpiece when the machining process takes place) [25]. Hence, it is desirable to have a methodology that can automatically filter the signal of interest. Traini et al. [12] recently utilized the change point detection approach to select the stationary window in which the machining process has been taken. However, the methodology proposed in this study is complex and accuracy dependent on a threshold parameter, α. In this work, a binary segmentation (BS) methodology that is threshold independent has been used to select a window in which the signal is stable (i.e., identifies the stationary phase of the machining activity), and no outliers are presented. The BS methodology identifies the window of a stable sensor signal based on the change in a time series signal's distributional properties. This methodology identifies change point in a time series, $y_{i=1:n} = \{y_1, y_2 \ldots\ldots y_n\}$ based on log-likelihood function for a normal distribution and which is defined as [26].

$$logL\left(\bar{y}, \sigma_0^2\right) = -\frac{n}{2} log\left(\sigma_0^2\right) - \frac{n}{2} log(2\pi) - \frac{0.5}{\sigma_0^2} \sum_{i=1}^{n} \left(y_i - \bar{y}\right)^2 \quad (1)$$

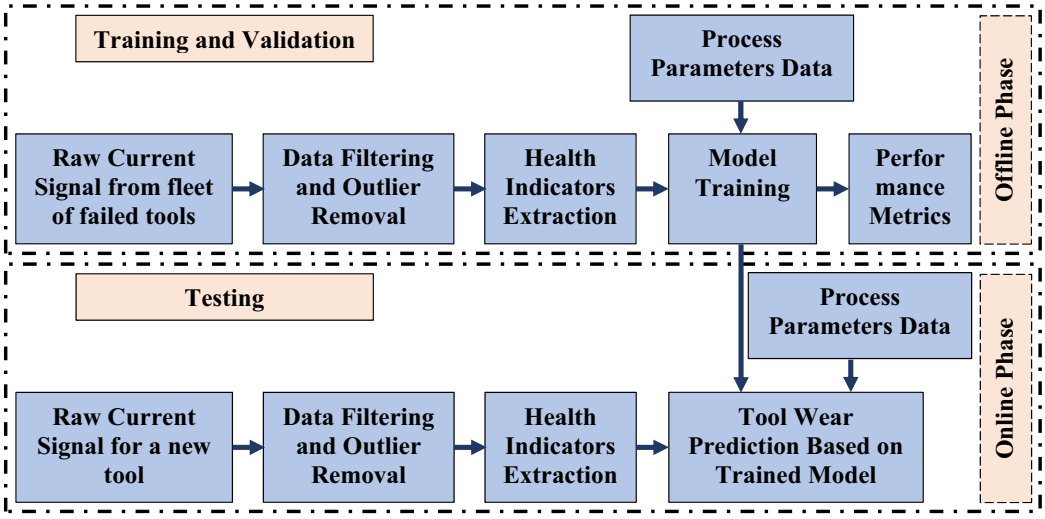

Fig. 1. Proposed framework for tool wear prediction.

where, $\overline{y}$ and σ_0^2 are the mean and variance of the time series, respectively.

The unknown parameters, $\overline{y}$ and σ_0^2, can be calculated by taking the partial derivative of the log-likelihood function with respect to the unknown parameters and setting it to zero.

$$\overline{y} = \frac{\sum_{i=1}^{n} y_i}{n} \tag{2}$$

$$\sigma_0^2 = \frac{\sum_{i=1}^{n} (y_i - \overline{y})^2}{n} \tag{3}$$

Eq. (1) can now be rewritten as

$$logL_0 = -\frac{n}{2}\left(log\left(2\pi\sigma_0^2\right) + 1\right) \tag{4}$$

The stable time-series signal window has been selected based on the change in log-likelihood value given in Eq. (4). The methodology assumes each data point of a time series as a change point and calculates the log-likelihood value for the datasets before the assumed change point and after the assumed change point. Both calculated log-likelihood values are added and then subtracted from the log-likelihood value calculated using complete time-series data as given below.

$$\lambda = \left[-\frac{k}{2}\left(log\left(2\pi\sigma_k^2\right) + 1\right) - \frac{n-k}{2}\left(log\left(2\pi\sigma_{n-k}^2\right) + 1\right) + \frac{n}{2}\left(log\left(2\pi\sigma_0^2\right) + 1\right)\right] \tag{5}$$

where, k represents the number of data points till change point c, and σ_k^2 and σ_{n-k}^2 is the variance of the k and rest $n-k$ data points, respectively.

This methodology can be defined as an optimisation problem. The location where a maximum change in this log-likelihood value is observed or the location at which test statistic λ reaches a maximum is considered as the location of the change point. One identified change point will generate two signal windows. The signal belong to these individual windows will be more stable compares to the complete signal.

To evaluate this methodology's performance in selecting a stable signal window, four normal distribution-based random time series with a mean of 100 and standard deviation (SD) of 1, 2, 4, and 6, respectively, containing 100 data points, are generated and joined as a single signal. The obtained simulated signal is shown in Fig. 2. Fig. 3(a) shows the window of stable signal identified using the proposed BS methodology. The BS methodology identifies a change point where the most significant change in distributional properties will be observed. Based on the simulated signal, the first change point is determined at data point number 200, as shown in Fig. 3(a). Two windows contain data points from 1 to 200, and 201 to 400 are identified using this methodology. However, the overall signal has four different windows of a stable signal.

This binary segmentation process could be repeated n number of times for $n + 1$ stable window selection. For the next window of stable

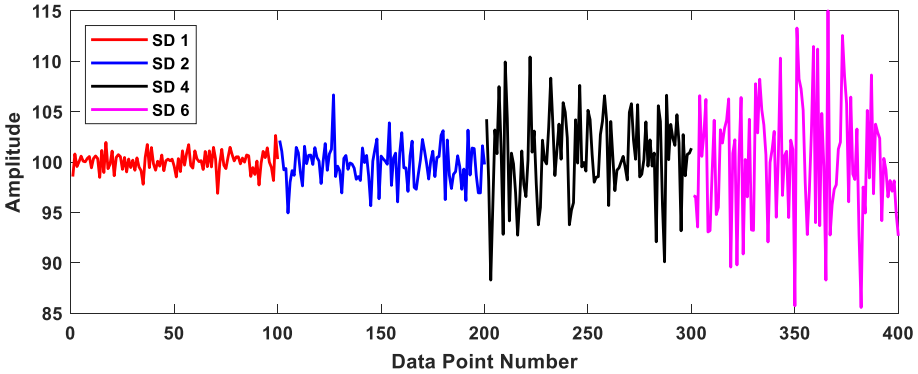

Fig. 2. Simulated normal distribution-based random time-series signal (red: mean 100, SD 1; blue: mean 100, SD 2; black: mean 100, SD 4; magenta: mean 100, SD 6). (For interpretation of the references to colour in this figure legend, the reader is referred to the web version of this article.)

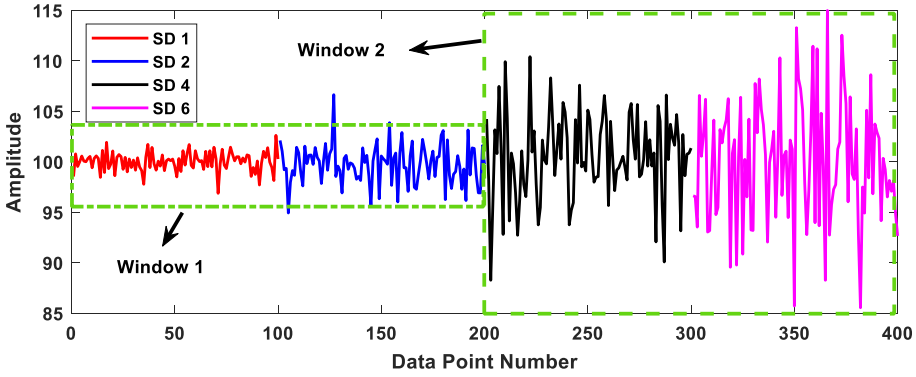

(a)

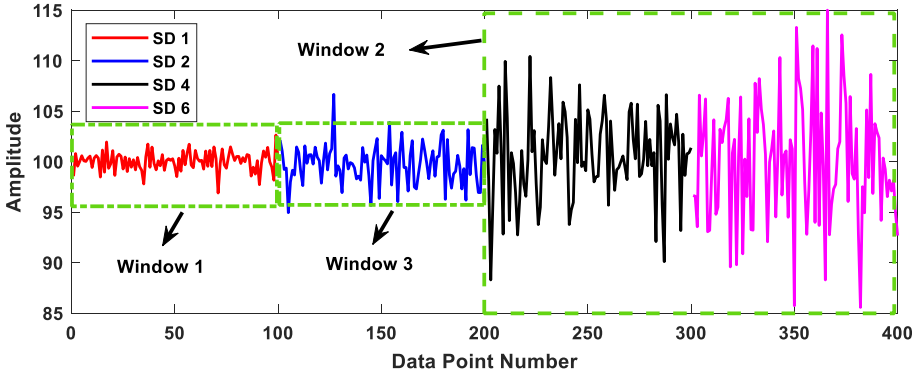

(b)

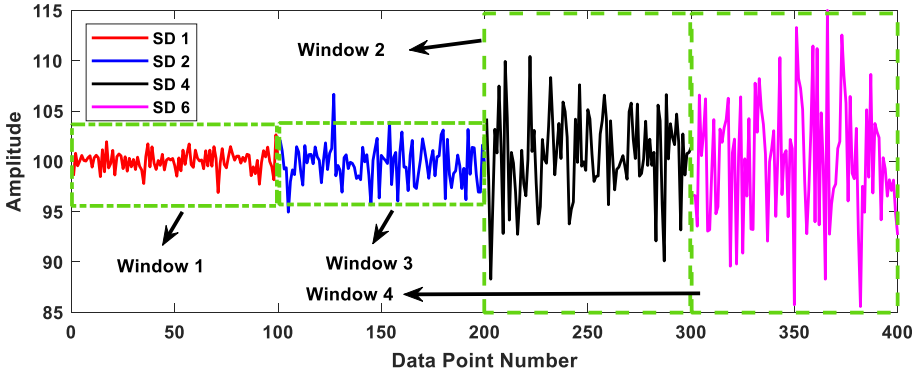

(c)

Fig. 3. Multiple windows of stable signal identification using the proposed BS methodology (a) two windows (b) three windows (c) four windows.

signal selection, the data points in windows obtained in the previous iteration will be treated separately. Hence for multiple windows identification, the test statistic λ given in Eq. (5) was applied separately to all previously identified segments. The segment in which the maximum value of test statistic λ is obtained was selected for new window formation. This process was iteratively applied unless desired segments are obtained or any given threshold criteria were met.

The location where test statistic λ achieves its maximum in any of the previous windows that will be considered as new window. Following this procedure, the third and fourth windows of a stable signal are identified, shown in Fig. 3(b) and (c), respectively. In actual application, a signal may contain multiple outliers, and hence this process could be repeated iteratively for n window selection of stable signal. The data-driven prediction model accuracy depends on the amount of data utilized for model building. It is important to have a large amount of data for the model-building to include all variability in the machining processes. Hence, the window which contains a maximum number of data points can be selected for further analysis.

This methodology automatically selects the window in which the machining sensor signal is almost stationary in one cycle of operation. The signal belongs to this window is further used for HI extraction and tool wear prediction.

2.2. *Health indicator for tool wear progression monitoring*

During the cutting tool and workpiece engagement, cutting energy is

released, resulting in the cutting forces [27,28]. The spindle motor current can indirectly measure these changes in cutting forces during tool-workpiece engagement as current is proportional to torque, which is proportional to cutting forces [29]. Increased tool wear increases the cutting forces, and the current drawn by the electric motors correspondingly also increases. However, the fault relevant information in the current signal is overlapped with disturbances from the other powered sources, which make it noisy and this will obstruct the detection of small fluctuations in the cutting force due to the tool wear [5]. In addition, the spindle power needed for material removal takes only a very small portion of the total power, while the rise of temperature which is inherent in motors under load will also affect this power consumption [30]. Thus, spindle current will be affected by these factors and hence is too complex to be interpreted directly. Hence HIs for tool wear monitoring have been extracted in the literature by analysing sensor signal in the time domain (TD), frequency domain (FD), and time-frequency domain (TFD) [31]. Some of the most widely used HIs in literature are shown in Table 1.

The HIs shown in Table 1 are extracted based on the overall behaviour of the raw current signal. The valuable information related to cutting tool degradation and dynamics is hidden in the signal. It is important to extract those pieces of information from the signal to reflect wear progression better. In this work, the HI for tool wear monitoring is formed based on the extraction of those useful pieces of information from the raw current signal. The raw current sensor signal has two main components: high-frequency carrier and low-frequency modulating signals. The carrier signal contains many frequencies irrelevant to the cutting tool degradation and also degradation relevant information masked by broadband noise. An increase in signal amplitude modulation has been observed with the degradation of the cutting tool. The signal gets modulated around the spindle's rotational speed, which can be seen in the signal envelope. Hence, this study aims to extract fault relevant information from the current signal utilizing signal envelope and discarding carrier signal. In previous studies [32,33], it has been shown that the envelope of the current sensor signals better diagnose the motor fault compared to the original raw current sensor signal. This study first time utilizes the envelope of the current sensor to more effectively monitor the wear progression.

A Hilbert transform approach is used for extracting the current signal envelope [34,35]. Hilbert transform is a time-domain convolution and mathematically can be expressed as

$$H[y(t)] = \frac{1}{\pi}\int_{-\infty}^{\infty}\frac{y(t)}{t-\tau}d\tau \tag{6}$$

where, $H[y(t)]$ is the Hilbert transform of time-domain current signal $y(t)$.

The magnitude of this complex time series represents the signal envelope and which can be extracted as

Table 1
Current sensor based HIs extracted for tool wear monitoring by various researchers.

References	Health indicators
[5]	TD: Mean FD: Mean TFD: Wavelet packet energy
[6]	TD: Root mean square, Variance, Skewness, Kurtosis, Peak, Peak-to-Peak FD: Peak-to-Peak, Spectral skewness, Spectral kurtosis TFD: Wavelet packet energy
[12]	TD: Max, Mean, RMS, Standard deviation, Skewness, Kurtosis, Peak-to-Peak, Crest factor FD: Max, Sum, Mean, Standard deviation, Skewness, Kurtosis, Relative spectral peak per band
[11]	TD: RMS, Kurtosis, Peak, Peak-to-Peak, Crest factor

$$a(t) = \sqrt{y^2(t) + H^2[y(t)]} \tag{7}$$

The extracted signal envelope $a(t)$ represents an estimate of the amplitude modulation present in the raw current signal.

For further enhancement in the enveloped signal's sensitivity, the enveloped signal is transformed to a different scale using the inverse hyperbolic cosine function. The inverse hyperbolic cosine function for the enveloped signal can be calculated as

$$cosh^{-1}[a(t)] = log\left[a(t) + \sqrt{a^2(t) - 1}\right] \tag{8}$$

Taking inverse hyperbolic cosine function for the enveloped signal produce HI with low scale and better correlation. The mean of the transformed enveloped signal ($cosh^{-1}[a(t)]$) is considered as the HI for wear monitoring. In summary, from Eqs. (6), (7), and (8), the proposed HI for wear monitoring can be presented as

$$Proposed\ HI = mean\left(log\left[\sqrt{y^2(t) + H^2[y(t)]} + \sqrt{y^2(t) + H^2[y(t)] - 1}\right]\right) \tag{9}$$

This proposed HI is further used for the online prediction of tool wear with a reliability-based Weibull Accelerated Failure Time Regression (WAFTR) model discussed in the next section.

2.3. Methodology for tool wear prediction

In this study, a reliability-based Weibull Accelerated Failure Time Regression (WAFTR) approach has been proposed for tool wear prediction. Weibull distribution is mainly used to analyse the reliability and maintainability of a component/system. The reliability function for this distribution is presented as [36].

$$R(t) = exp\left(-\left(\frac{t}{\eta}\right)^{\beta}\right) \tag{10}$$

where, η is the scale or characteristics life parameter, i.e., time at which 63.2 % of failure occurs, and β is the shape parameter. $R(t)$ presents the probability that component-time to failure, i.e., T will be greater than or equal to some time period t, i.e., $Pr\{T \geq t\}$.

In the present work, the machine tool assumes to be failed if tool wear in the current state is greater than the critical wear value. Hence, the current problem's reliability function will represent the probability that the flank tool wear in the current state of the tool is lesser than or equal to the critical value. By considering tool wear as a life parameter, the reliability formula mathematically for the present problem can be presented as

$$Pr(wear \leq wear_{critical}) = exp\left(-\left(\frac{wear}{\eta}\right)^{\beta}\right) \tag{11}$$

The tool life depends on the process parameters such as feed rate, depth of cut (DOC), spindle speed, and tool and work materials, etc. These parameters also affect job duration, quality, and accuracy of finished product and production cost. All these parameters are termed external parameters or external covariates. The cutting tool's degradation leads to change in characteristics such as vibration, AE, the cutting force generated, current signal drawn by machine tool, etc. The parameters that indirectly represent or used for tool conditions are termed as internal parameters or internal covariates. These external and internal covariates should be part of a prediction model for an accurate, reliable, and online tool condition assessment. Hence, the scale parameter in a Weibull distribution could be modified and expressed as a function of external/internal covariates and termed as Weibull Accelerated Failure Time Regression (WAFTR) model. The WAFTR model for the present machine tool wear prediction model can be expressed as

$$Pr(wear \le wear_{critical}) = exp\left(- \left(\frac{wear}{exp^{a_o + \sum_{l=1}^{q} a_l I_l + \sum_{j=1}^{m} b_j E_j}} \right)^{\beta} \right) \tag{12}$$

where, *I and E* represent internal and external covariates respectively, *q and m* represent the number of internal and external covariates respectively, a_o is the intercept, a_l is the regression coefficient for l^{th} internal covariate and b_j is the regression coefficient for j^{th} external covariate.

The Eq. (12) in the expanded form can be represented as

$$R(wear \le wear_{critical}) = exp\left(- \left(\frac{wear}{exp\left[a_o + \left(a_1 I_1 + a_2 I_2 \ldots\ldots\ldots\ldots + a_q I_q\right) + \left(b_1 E_1 + b_2 E_2 \ldots\ldots\ldots\ldots + b_m E_m\right)\right]} \right)^{\beta} \right) \tag{13}$$

Based on the available condition monitoring sensor data and life-affecting external covariates, the value of the unknown parameters such as β, a_o, a_1, b_1, etc. given in Eq. (13) can be estimated using the maximum likelihood estimation (MLE) approach. In generalised form, the likelihood function can be defined as

$$L\left(\beta, a_o, a, b\right) = \prod_{d=1}^{g} f(wear_d, I_d, E_d) \times \prod_{s=1}^{p} R(wear_s, I_s, E_s) \tag{14}$$

where, *d* and *s* are indexes for the number of failure and suspension/degradation data points respectively and $f(wear_d, I_d, E_d)$ is the probability density function for WAFTR model. Eq. (14) in the expanded form can be represented as

$$\begin{aligned} L\left(\beta, a_o, a_1, a_2, \ldots\ldots\ldots, a_q, b_1, b_2, \ldots\ldots\ldots, b_m\right) = & \prod_{d=1}^{g} \frac{\beta}{\left(exp\left(a_o + a_1 I_{1d} + a_2 I_{2d} \ldots\ldots\ldots\ldots + a_q I_{q_d} + b_1 E_{1d} + b_2 E_{2d} \ldots\ldots\ldots\ldots + b_m E_{md}\right)\right)^{\beta}} (wear_d)^{\beta-1} \\ & \times exp\left[- \left(\frac{wear_d}{exp\left(a_o + a_1 I_{1d} + a_2 I_{2d} \ldots\ldots\ldots\ldots + a_q I_{q_d} + b_1 E_{1d} + b_2 E_{2d} \ldots\ldots\ldots\ldots + b_m E_{md}\right)} \right)^{\beta} \right] \\ & \times \prod_{s=1}^{p} exp\left[- \left(\frac{wear_s}{exp\left(a_o + a_1 I_{1s} + a_2 I_{2s} \ldots\ldots\ldots\ldots + a_q I_{q_s} + b_1 E_{1s} + b_2 E_{2s} \ldots\ldots\ldots\ldots + b_m E_{ms}\right)} \right)^{\beta} \right] \end{aligned} \tag{15}$$

The partial derivative of the Eq. (15) with respect to the unknown parameters β, a_o, a_1, a_2, ……, a_q, b_1, b_2, ……, b_m and setting the derivative equal to zero will give optimal value for these unknown parameters. It is very crucial to know what the models have learned, particularly in real-world situations where decision reliability is important. The interpretability increases model acceptance. Unlike other machine learning models such as ANN, SVM, etc., WAFTR is a white box modeling approach and fully interpretable. The WAFTR model is fully interpretable in two ways, i.e., gives acceleration factor for different levels of covariate and covariates importance.

Eq. (13) provides coefficients for covariates and can infer how particular HI is affecting tool wear. For example, in WAFTR, the survival time (e.g. wear in the present case) accelerates or decelerates by a constant factor when comparing different levels for a particular covariate. The coefficients of the covariates help in estimating this constant factor. The negative coefficient value indicates that an increase in particular covariate level will deaccelerate tool wear and vice versa for a positive value. Hence, in WAFTR, the effect of covariate is multiplicative on wear, and it is said to "accelerate/deaccelerate" wear rate, which can be mathematically explained below.

From Eq. (13), the scale parameter η for WAFTR can be presented as [37–39].

$$\eta = exp\left[a_o + \left(a_1 I_1 + a_2 I_2 \ldots\ldots\ldots\ldots + a_q I_q\right) + \left(b_1 E_1 + b_2 E_2 \ldots\ldots\ldots\ldots + b_m E_m\right)\right] \tag{16}$$

Keeping other covariates values fixed, increase covariate I_1 value by x unit from I_1 to $I_1 + x$ and denote this scale parameter as η_2

$$\eta_2 = exp\left[a_o + \left(a_1 (I_1 + x) + a_2 I_2 \ldots\ldots\ldots\ldots + a_q I_q\right) + \left(b_1 E_1 + b_2 E_2 \ldots\ldots\ldots\ldots + b_m E_m\right)\right] \tag{17}$$

From Eqs. (16) and (17), the η_1 and η_2 parameters are related as

$$\eta_2 = e^{x a_1} \eta_1 \tag{18}$$

The factor $e^{x a_1}$ in Eq. (18), represent the acceleration factor (AF) for particular levels of covariates and hence evaluate the effect of covariate levels on the tool wear. For example, x unit increase in covariate level, the AF can be interpreted as effects on wear, which can either accelerate (AF greater than 1) or deaccelerate (AF less than 1) wear.

It is crucial to determine the most suitable external and internal covariates statistically in the model. The covariate selection in WAFTR model is made using a backward elimination procedure by selecting the covariates with the lowest *p*-value. The *p*-value is the probability of obtaining sample results using the chi-square test, assuming the null hypothesis is correct. In WAFTR model, the null hypothesis assumes no relationship between the covariate and tool wear and vice-versa for the

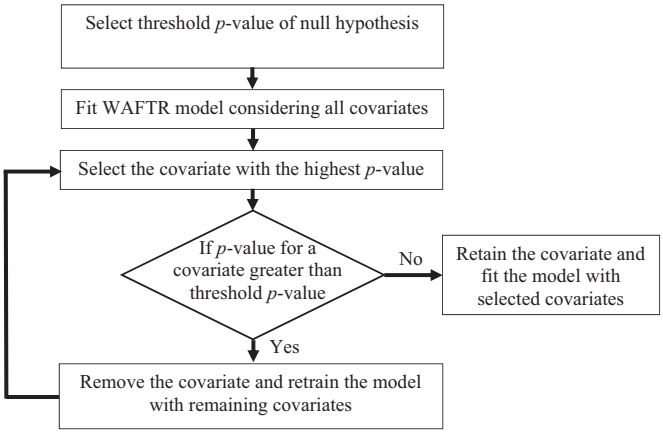

Fig. 4. Backward elimination procedure for covariates selection in WAFTR model

alternate hypothesis. A lower *p*-value indicates that the alternate hypothesis is correct, and the null hypothesis is not true. The choice of selecting the threshold *p*-value is arbitrary. Most of the researchers used the *p*-values as 0.05, 0.01 and 0.001. A lower p-value indicates particular covariates/features/HIs selected are highly significant for model formation. Hence, a lower p-value of 0.01 is chosen in this study, i.e. which indicated only a 1 % probability that the results (i.e., covariates selected) are due to random chance.

Table 2
Experimental conditions for different experiments.

Experiment/cutter number	Depth of cut (in mm)	Feed rate (in mm)	Tool material	Number of cycles
1	1.5	0.5	Cast Iron	17
2	0.75	0.5	Cast Iron	14
3	0.75	0.25	Cast Iron	16
4	1.5	0.25	Cast Iron	7
5	1.5	0.5	Steel	6
6	1.5	0.25	Steel	1
7	0.75	0.25	Steel	8
8	0.75	0.5	Steel	6
9	1.5	0.5	Cast iron	9
10	1.5	0.25	Cast iron	10
11	0.75	0.25	Cast iron	23
12	0.75	0.5	Cast iron	15
13	0.75	0.25	Steel	15
14	0.75	0.5	Steel	10
15	1.5	0.25	Steel	7
16	1.5	0.5	Steel	6

For best covariate selection, first, WAFTR model is fitted using all covariates in the model, and the covariate with the highest *p*-value is identified. The identified covariate will be removed if the *p*-value for this covariate is greater than the threshold value. The model is retrained using the remaining HIs. The non-significant HIs are removed, sequentially repeating this procedure one by one and termed backward elimination procedure for most suitable covariate selection. This procedure is repeated until all covariates considered in the model have a *p*-value less than 0.01. Fig. 4 shows the backward elimination procedure for covariates selection.

3. Data set for proposed framework performance validation

The milling datasets provided by NASA AMES and the University of Berkeley [40] have been used for performance validation of the proposed framework for tool wear prediction. The experiments were performed at 16 different conditions. Table 2 shows details of the experiment's conditions at which these sixteen experiments were performed.

The cutting speed in all experiments was constant, which is equal to 200 m/min. Four different types of sensor data, such as acoustic emission, vibration, DC current and AC current, were collected to monitor machine tool wear progression. However, this study is restricted to use spindle AC current sensor data for tool wear monitoring, and hence data from this sensor is only further discussed. A 70 mm diameter face mill with six inserts (type KC710) was used for machining operation. The inserts are coated with multiple titanium carbide layers, titanium carbonitride, and titanium nitride in sequence. The machining operation using this milling cutter is done to machine a workpiece of size 483 *mm* × 178 *mm* × 51 *mm*. The flank wear on the insert was measured in each cycle with the help of a microscope.

Fig. 5 shows tool wear progression with the number of cycles for different cutters. The data set for cutter number 6 is not completely available and hence not considered in this study. In addition, the tool flank wear was not measured in every cycle, and therefore no flank wear data is available for 21 instances. A total of 167 instances were available. After eliminating 21 instances for which tool wear data is not available and cutter 6 data, a total of 145 instances remained for model development and validation. Based on the current signal sensor data collected from such 145 instances, the following section shows the wear prediction results obtained using the proposed framework for machine tool wear monitoring explained in Section 2.

4. Results and discussions

This section shows the performance of binary segmentation-based

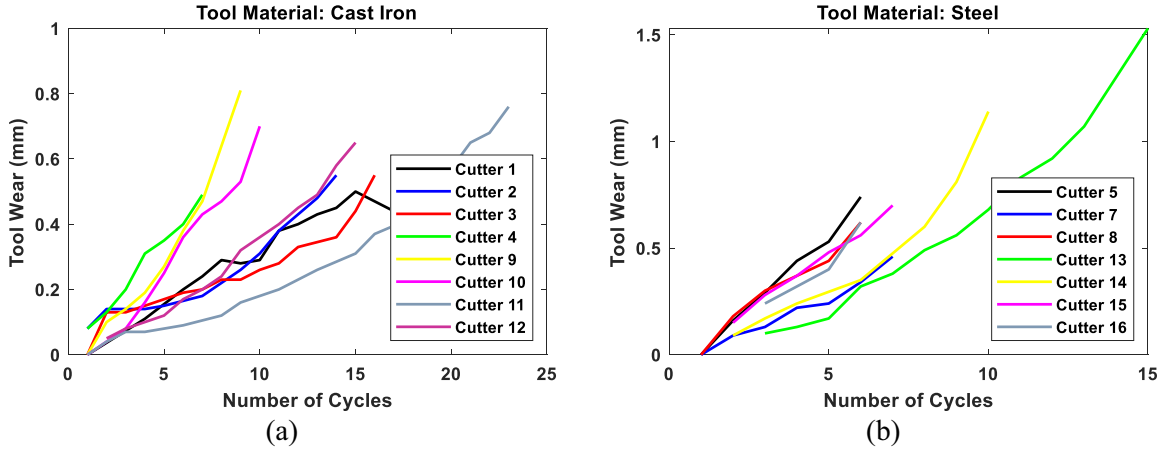

Fig. 5. Tool wear progression with a number of cycles for cutters made of (a) cast iron (b) steel.

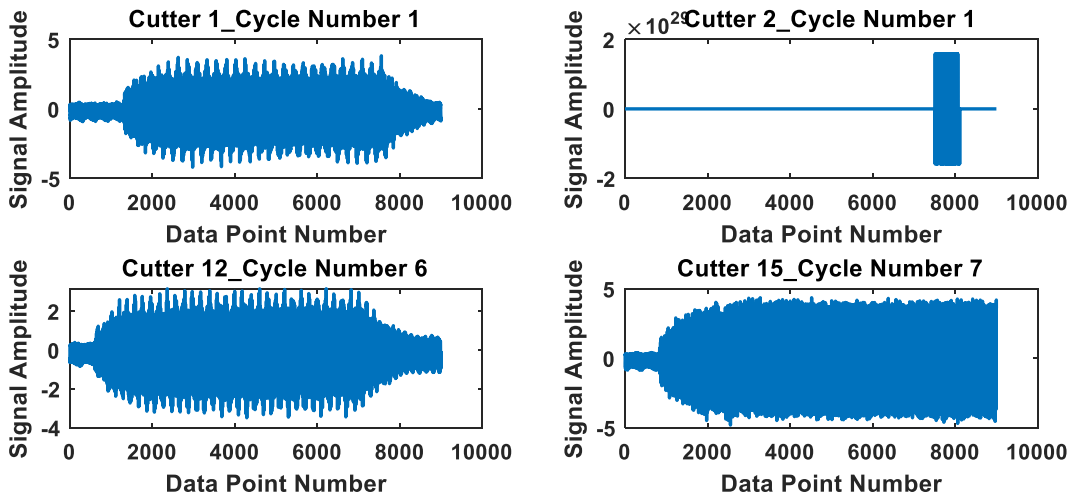

(a)

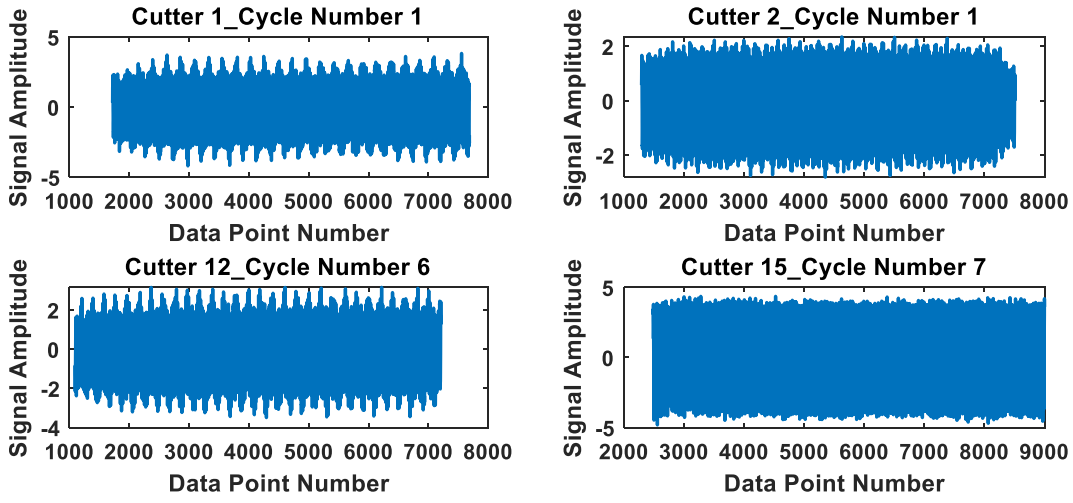

(b)

Fig. 6. (a) Raw signal obtained from current sensor signal (b) stable signal of interest obtained using proposed BS methodology.

data filtering and outlier removal methodology, proposed HI utilizes mean of inverse hyperbolic cosine function fitted to the signal envelope and WAFTR based wear prediction methodology using data sets discussed in Section 3.

4.1. Data filtering and outlier removal

Each current signal from 145 instances contains 9000 data points, and a few current signal data obtained for different experiments is shown in Fig. 6(a). The amplitude of the current signal obtained in this study is very high/low at the start and end of the machining process, maybe because the tool is not in constant contact with the workpiece when the machining process takes place. In a few cases, erratic signal behaviour is also observed, for example, the signal shown for cutter 2 in Fig. 6(a). It is desirable to select the window in which the signal has stable behaviour. Hence, BS methodology has been applied for the window selection. Fig. 6(b) shows the signal obtained after the proposed BS methodology applied on current sensor data, demonstrating for different types of the obtained current signal how effectively the proposed BS methodology can identify the window when the machining sensor signal is stable. For example, for signal belong to the first cycle of cutter number 1, from Fig. 6(a), the stable signal behaviour is observed between data points 1800 to 7500, which is identified using the proposed BS methodology as shown in Fig. 6(b). The stable signal obtained using the proposed BS methodology has been further used for HIs extraction and tool wear prediction.

4.2. Health indicator performance

A prediction model's performance depends on the sensitivity of the HIs to represent the cutting tool degradation [41]. The proposed HI in this work is based on the envelope of the raw current signal. Fig. 7 shows the original current signal and envelope of the same, which is calculated using Eq. (7). As discussed earlier, the wear on the cutting tool modulates the current signal. This modulation which is extracted based on the signal envelope, is expected to increase as tool wear increases. The inverse hyperbolic cosine function of the enveloped signal is taken to enhance the signal sensitivity further. The mean of the enhanced enveloped signal represents the HI for tool wear monitoring.

Fig. 8(a) shows the variation of the proposed HI for different cutters. Corresponding wear values are plotted in Fig. 8(b). In most instances, the HI value increases as tool wear increases. The proposed HI

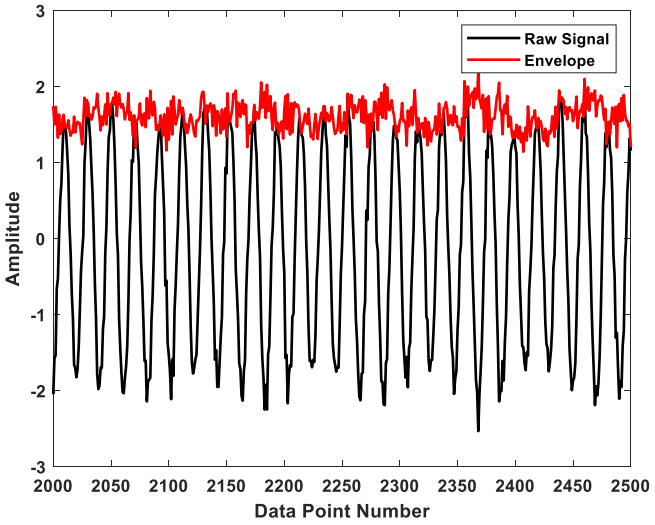

Fig. 7. Signal enveloping.

performance is compared with existing HIs based on the correlation of particular HI with tool wear progression. From Table 1, a total of 32 most used current sensor based HIs for tool wear monitoring are considered. Out of these HIs, eight were extracted in time-domain (mean, maximum, sum, standard deviation (SD), skewness, root mean square (RMS), peak-to-peak (P2P), and crest factor (CF)), eight were extracted in frequency-domain (mean, maximum, sum, SD, skewness, kurtosis, P2P and relative spectral peak per band (RSPB)), and 16 were extracted in time-frequency (4 level wavelet packet energy (WE)) domain. The correlation coefficient (CC) obtained for existing HIs and proposed HI with wear is reported in Table 3. From Table 3, compares to existing HIs (HI number 1 to 32), the highest correlation value is obtained for the proposed HI (HI number 33), which is 0.63. Hence, this HI is further used for tool wear prediction. The performance of the proposed HI and existing HIs is also shown with the help of tool wear prediction results, which will be discussed in the next section.

4.3. Tool wear prediction results

As discussed earlier in Section 3, a total of 145 instances are available for validation of the proposed methodology. Leave one out cross-validation (LOOCV) approach has been used to evaluate the proposed tool wear prediction framework. The WAFTR model discussed in Section 2.3 is used for tool wear prediction based on the proposed HI shown in Section 4.2. For the present problem, the external covariates will be process parameters such as depth of cut (DOC), feed rate and tool material and internal covariates will be current sensor-based extracted HIs for tool wear prediction. Initially, all process-related information is combined with the current sensor-based extracted HIs to improve prediction performance as cutting tools made of different materials and run under variable operating conditions. In addition, cutting tool running time cycle (run and time) information also has been considered in the model. After considering all these covariates, the WAFTR model for the current problem can be presented as

Fig. 9 shows tool wear prediction results. The proposed WAFTR model accurately predicted tool wear except for a few instances where actual tool wear is predominately high in cutter numbers 9 and 13–16. The model parameters estimated based on other cutters' data doesn't show high tool wear corresponding to the particular operating conditions. Due to limited available data in this study for model development, it is very difficult to develop a robust model that can accurately predict wear in all scenarios. The availability of more training data points can be helpful in further reducing the prediction error. In addition, cutter number 16 has data only for three cycles, and hence we can't comment on prediction results for this cutter due to data inefficiency.

To further evaluate the performance of the proposed HI, the wear prediction results are obtained when other existing HIs are considered in the WAFTR model. The percentage error in prediction is calculated to evaluate the proposed WAFTR model's performance when using existing HIs and the proposed HI. The obtained prediction error results are reported in Table 4.

From Table 4, the percentage error in tool wear prediction is minimum (20.8 with HI 33) with proposed HI compares to existing HIs (in existing HIs, best results are obtained with HI 6, which is 25.4). This shows the proposed HI is useful for better tool wear prediction. In addition, the above analysis is repeated for different existing wear prediction models such as RFR and ANN to benchmark the performance of the proposed WAFTR wear prediction model. A total of 500 decision trees were used in the RFR model, and an ANN model with one hidden layer and 20 neurons were used. The tool wear prediction results obtained with these three models are illustrated in Fig. 10. It shows that the tool wear prediction results obtained using the proposed WAFTR model are closer to the actual wear value than the RFR and ANN models. Table 5 shows the percentage error in prediction obtained using all three models. Overall, the percentage error in prediction obtained using the proposed WAFTR model is 20.8 %, whereas it is 26.8 % and 44.8 % using RFR and ANN model, respectively. This shows the proposed WAFTR model outperforms the existing machine learning models such as RFR and ANN for tool wear prediction.

4.3.1. WAFTR interpretation

The WAFTR model has the advantage of having two separate interpretations, i.e., acceleration factor and inbuilt most suitable covariates selection capability. Based on the backward elimination procedure explained in Fig. 4, the relative importance of all internal (HIs given in Table 4 and running time cycle (run and time) information) and external covariates (DOC, feed rate and material type) is calculated and ranked according to their importance in Fig. 11. The higher p-value, the lower the importance is. From Fig. 11, among the internal covariates, the WE12 HI extracted in the time-frequency domain is the least suitable HI (p-value = 0.89) and the proposed HI is the most suitable HI (p-value = 6.52e-39). Among the external covariates, material type (p-value = 0.03) is least suitable and DOC (p-value = 2.30e-27) and feed rate (p-value = 4.09e-47) are most suitable. In addition, none of cutting tool running time cycle information (i.e., run (p-value = 0.66), time (p-value = 0.04)) is important in the model. In summary, the p-value obtained for the proposed HI and external covariates DOC and feed rate is less than 0.01. Hence, these covariates are only retained in the model for wear prediction and now the WAFTR model can be presented as

$$Pr(wear \le wear_{critical}) = exp\left(-\left(\frac{wear}{exp[a_o + (a_1{*}run + a_2{*}time + a_3{*}propsoed\ HI) + (b_1{*}DOC + b_2{*}feed\ rate + b_3{*}material)]} \right)^{\beta} \right) \quad (19)$$

$$Pr(wear \le wear_{critical}) = exp\left(- \left(\frac{wear}{exp[a_o + (a_1{*}propsoed\ HI) + (b_1{*}DOC + b_2{*}feed\ rate)]} \right)^{\beta} \right) \quad (20)$$

Based on the most suitable selected internal (i.e., proposed HI) and external covariates (i.e., DOC and feed rate), the ANN and RFR model's performance have also been investigated and compared with WAFTR model. Fig. 12 shows the tool wear prediction results obtained using all three models when non-significant covariates are removed. Comparing with Fig. 10, the prediction results by RFR and ANN models have been apparently affected by the running time cycle information. In contrast, the performance of the proposed WAFTR model is almost similar with and without consideration of the running time cycle information. Table 6 shows the percentage error in prediction obtained using all three models when non-significant covariates are removed. Overall, the percentage error in prediction obtained using the proposed WAFTR model is 20.4 %, whereas it is 65.2 % and 160.5 % using RFR and ANN models, respectively. This indicates that the proposed WAFTR model can also accurately predict tool wear with limited process information, highlighting another advantage of the proposed model compared to existing machine learning-based models.

Another advantage of WAFTR model is it provides an acceleration factor (AF). The AF estimated using the WAFTR model can help in deaccelerating the wear by controlling the covariate levels. For example, for cutter number 2, the experiment was performed at a DOC and feed rate of 0.75 and 0.5, respectively. Based on the LOOCV approach, for this cutter, the WAFTR model eq. is shown below

$$Pr(wear \le wear_{critical}) = exp\left(- \left(\frac{wear}{exp[-2.14 + (1.99{*}Propsoed\ HI) + (-1.11{*}DOC - 2.48{*}feed\ rate)]} \right)^{4.56} \right) \quad (21)$$

From Eq. (21), the external covariates, i.e., DOC and feed rate levels, can be adjusted to deaccelerate the wear progression. The negative coefficient values for DOC and feed rate show that increased levels for both these two external covariates will deaccelerate the wear progression. How much wear will deaccelerate can be quantified using the acceleration factor. For example, if DOC for this cutter is increased from 0.75 to 1.5, the AF ($e^{0.75*-1.11} = 0.43$; from Eqs. (18) and (21)) will be 0.43. This indicates tool wear for this cutter can be reduced 0.43 times if DOC increases from 0.75 to 1.5. This shift (black line for DOC 0.75 to red line for DOC 1.5) in wear progression can be seen from Fig. 13(a). Similarly, if the feed rate decreased from 0.5 to 0.25, the AF ($e^{-(0.25*-2.48)} = 1.86$; from Eq. (18) and (21)) will be 1.86. A decrease in feed rate increases the wear 1.86 times which can be seen from Fig. 13(b) (black line for feed rate 0.5 to blue line for feed rate 0.25). If DOC increased from 0.75 to 1.5 and the feed rate decreased from 0.5 to 0.25, the AF $e^{0.75*-1.11+0.25*2.48)} = 0.81$) will be 0.81 (shift in wear progression from black line to magenta line in Fig. 13(a)). The acceleration factors obtained for increase/decrease in DOC and feed rate for cutter number 2 is reported in Table 7. Similar results for cutter number 10 can be seen in Fig. 13(b) and Table 8. In summary, the acceleration factor provided by WAFTR model can be used to control (accelerating and deaccelerating) the tool wear by adjusting levels of the covariate.

From Eq. (21), the WAFTR model has five coefficients, i.e., a_o, a_1, b_1, b_2, and β. Fig. 14 shows the variation of these coefficients for different training data combinations. The intercept, HI coefficient, DOC coefficient, feed rate coefficient, and shape parameter value lies in the range of −2.18 to −2.11, 1.97 to 2.02, −1.14 to −1.08, −2.55 to −2.43, and 4.55 to 4.69, respectively. Very little variation (standard deviation for intercept, HI coefficient, DOC coefficient, feed rate coefficient, and the shape parameter value is obtained 0.008, 0.005, 0.006, 0.01, and 0.024, respectively) in coefficient values for different training data combinations indicates the model consistency.

In summary, the BS and WAFTR models presented in this study are very generic and can also be implemented for different precision machines. For example, in all precision machines, the cutting tool may not constantly contact the workpiece all the time during machining. The BS methodology will be helpful in such scenarios for identifying the stationary phase of the machining activity in each cycle of operation. In all precision machines, the cutting tool generally operates under variable operating conditions for machining different materials. The WAFTR model will be helpful in such scenarios for estimating the tool wear progression for different tool/workpiece material and change in the levels of the process parameters.

5. Conclusion

This study proposed a unified, systematic, and generic framework that can be applied to different machining processes for tool wear prediction. The proposed framework contributes to three directions (i.e., data filtering and outlier removal, sensitive HI extraction and fully interpretable tool wear prediction model) for tool wear prediction.

- A binary segmentation methodology was proposed for data filtering and outlier removal. The obtained sensor data may have random or known fluctuations in signal. The proposed binary segmentation methodology significantly selected the window in which the signal was more stable. The signal that belongs to this stable window was further selected for health indicator extraction and tool wear prediction model development.
- The modulation in the current signal increased with an increase in tool wear. Hence modulation characteristics of the current signal were extracted based on the envelope of the signal. The inverse hyperbolic cosine function was fitted to the enveloped signal for further enhancement in the signal sensitivity. The mean of the modified enveloped signal represented tool wear progression better than existing HIs for tool wear monitoring.
- A WAFTR model was proposed to predict tool wear based on the extracted health indicator. The performance of the proposed model was compared with existing models such as RFR and ANN. The proposed WAFTR model performance considering the proposed health indicator was observed better than existing HIs and existing models for tool wear prediction.
- In addition, the WAFTR model has better interpretability than existing ML models. The WAFTR model provided a functional relationship between the tool wear, HIs and machine process parameters. It could be inferred which process parameters are accelerating

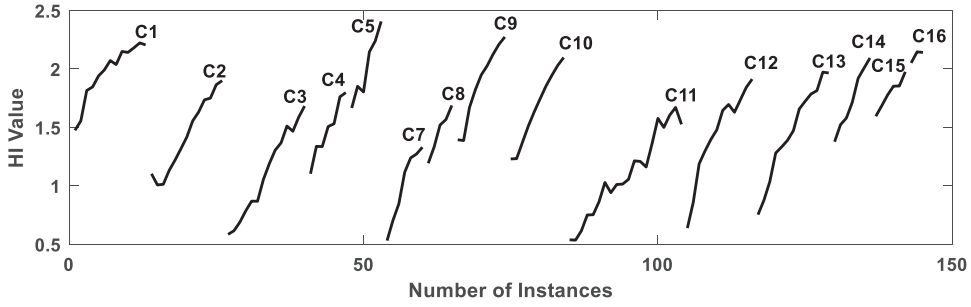

(a)

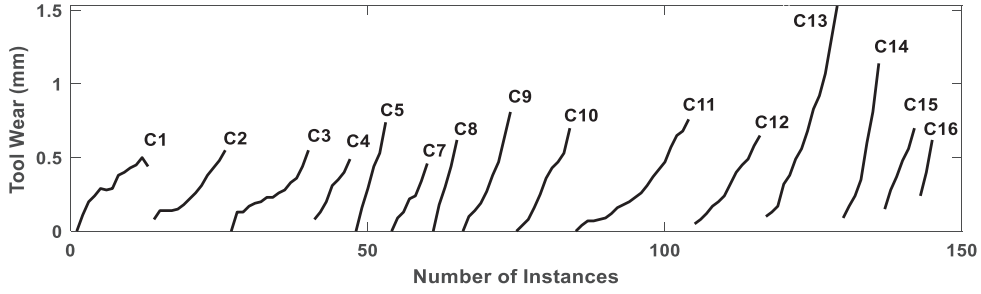

(b)

Fig. 8. (a) Proposed HI variation for different cutters (b) Wear progression for different cutters.

Table 3
CC value obtained for existing HIs and proposed HI.

TD based								
HI number	1	2	3	4	5	6	7	8
HI name	Mean	Maximum	Sum	SD	Skewness	RMS	P2P	CF
CC value	0.45	0.60	0.39	0.60	0.2	0.60	0.59	0.53
FD based								
HI number	9	10	11	12	13	14	15	16
HI name	Mean	Maximum	Sum	SD	Skewness	Kurtosis	P2P	RSPB
CC value	0.51	0.56	0.53	0.59	0.27	0.29	0.56	0.18
TFD based								
HI number	17	18	19	20	21	22	23	24
HI name	WE1	WE2	WE3	WE4	WE5	WE6	WE7	WE8
CC value	0.62	0.42	0.58	0.58	0.48	0.57	0.45	0.49
HI number	25	26	27	28	29	30	31	32
HI name	WE9	WE10	WE11	WE12	WE13	WE14	WE15	WE16
CC value	0.002	0.37	0.04	0.24	0.20	0.49	0.05	0.56
Proposed								
HI number					33			
HI name					Mean of inverse hyperbolic cosine function fitted to signal envelope			
CC value					0.63			

or deaccelerating the tool wear in terms of an acceleration factor by controlling the levels of a particular process parameter. Hence, the tool wear evolution could be deaccelerated or minimised. In addition, WAFTR model automatically selected the most suitable process parameters and HIs. Using the chi-square test, the model backwardly eliminated the process parameters and HIs, which would not be significant for tool wear monitoring.

Since the WAFTR model has inbuilt most suitable HI selection capability and hence can also be used to select the most suitable sensors for tool wear monitoring. This process will help in minimising the sensors required for tool condition monitoring and can help in reducing the cost associated with a number of sensors.

The proposed method relies on historical data from all operating conditions to establish an accurate estimation of model parameters. It

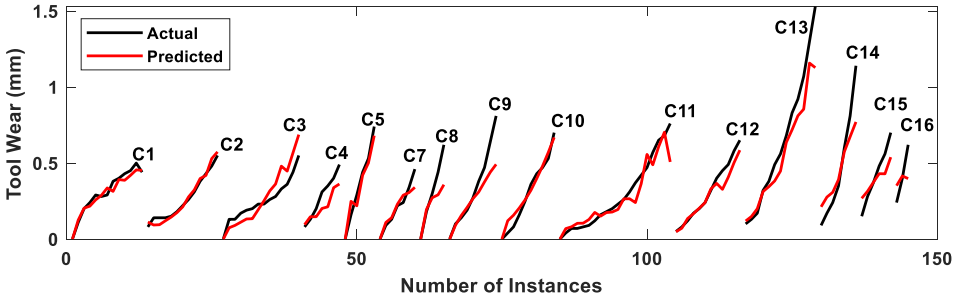

Fig. 9. Tool wear prediction results obtained using the proposed tool wear prediction framework.

Table 4
Percentage error in tool wear prediction obtained using existing HIs and proposed HI.

HI number	HI 1	HI 2	HI 3	HI 4	HI 5	HI 6	HI 7	HI 8	HI 9
Correlation	29.04	26.02	29.68	25.7	32.04	25.4	25.9	30.3	31.07
HI number	HI 10	HI 11	HI 12	HI 13	HI 14	HI 15	HI 16	HI 17	HI 18
Correlation	27.4	30.8	26.8	31.6	26.8	27.4	31.6	27.6	31.3
HI number	HI 19	HI 20	HI 21	HI 22	HI 23	HI 24	HI 25	HI 26	HI 27
Correlation	30.9	28.11	30.5	27.2	31.7	30.9	30.7	30.8	31.5
HI number	HI 28	HI 29	HI 30	HI 31	HI 32	HI 33			
Correlation	31.3	31.4	29.8	31.3	28.7	20.8			

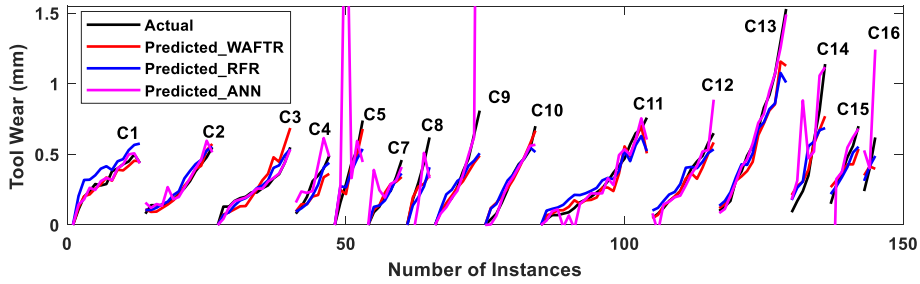

Fig. 10. Tool wear prediction results obtained using WAFTR, RFR, and ANN models.

Table 5
Percentage error in tool wear prediction obtained using WAFTR, RFR, and ANN models.

Model name	WAFTR	RFR	ANN
% error in prediction	20.8	26.8	44.8

can provide very accurate results for operating conditions that fall within the range used for model training. In addition, prediction errors are high for a few cutters when predominately tool wear was high compared to other cutters. The model parameter updating strategy may resolve this issue. Future work will be focused to overcome these shortcomings of the WAFTR model.

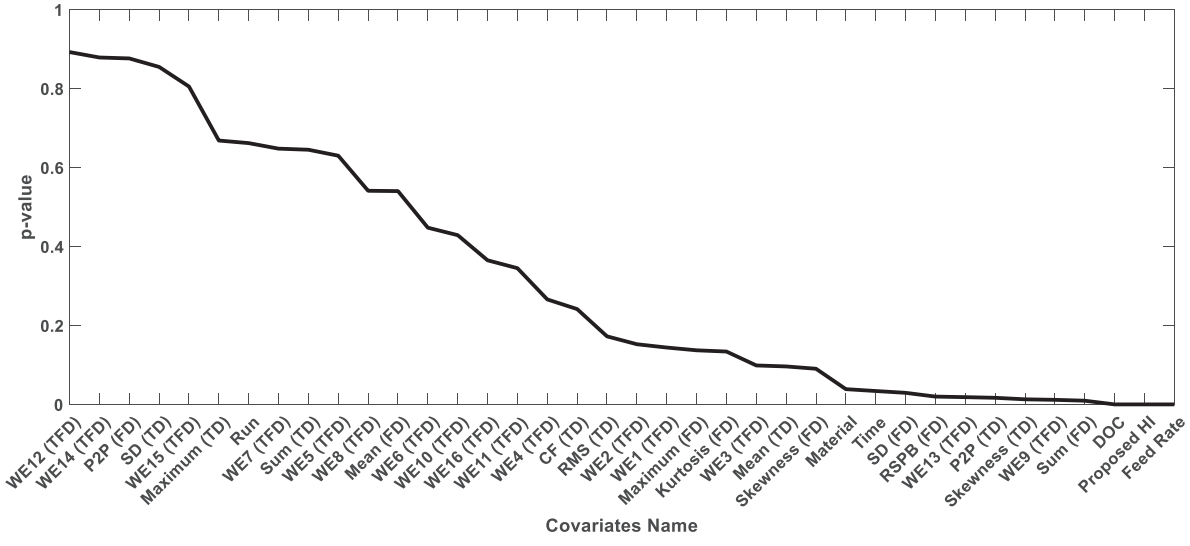

Fig. 11. Relative importance of covariates.

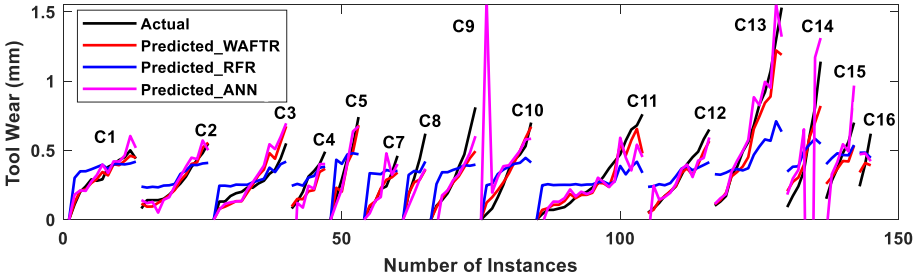

Fig. 12. Tool wear prediction results obtained using WAFTR, ANN, and RFR models when non-significant covariates identified based on WAFTR model are removed.

Table 6
Percentage error in tool wear prediction obtained using WAFTR, RFR, and ANN models when non-significant covariates identified based on WAFTR model are removed.

Model name	WAFTR	RFR	ANN
% error in prediction	20.4	65.2	160.5

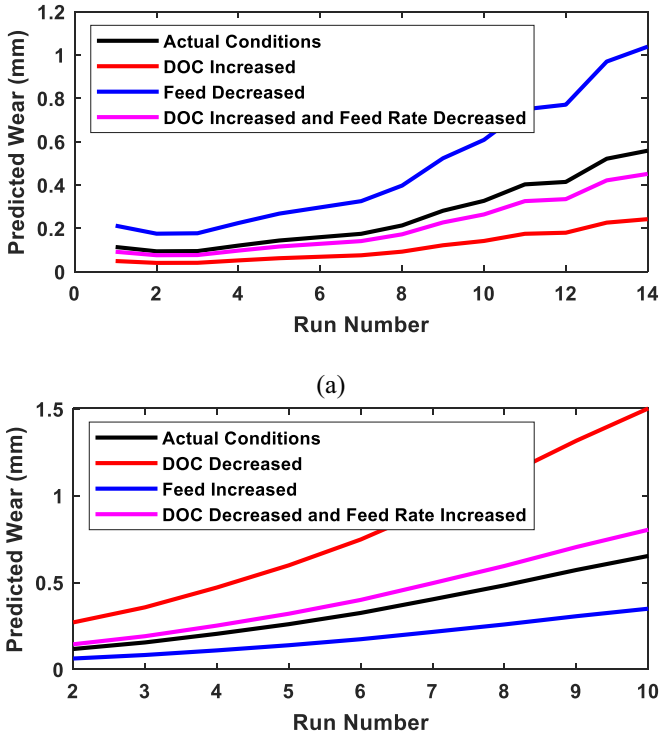

Fig. 13. Tool wear prediction results when process parameters are changed for the cutter number (a) 2 (b) 10.

Table 7
Acceleration factor calculation using WAFTR model for cutter number 2.

Actual DOC (0.75) and feed rate (0.5)	DOC increased from 0.75 to 1.5	Feed rate decreased from 0.5 to 0.25	DOC increased from 0.75 to 1.5, and the feed rate decreased from 0.5 to 0.25
1	0.43	1.86	0.81

Table 8
Acceleration factor calculation using WAFTR model for cutter number 10.

Actual DOC (1.5) and feed rate (0.25)	DOC decreased from 1.5 to 0.75	Feed rate increased from 0.25 to 0.5	DOC decreased from 1.5 to 0.75, and the feed rate increased from 0.25 to 0.5
1	2.30	0.54	1.23

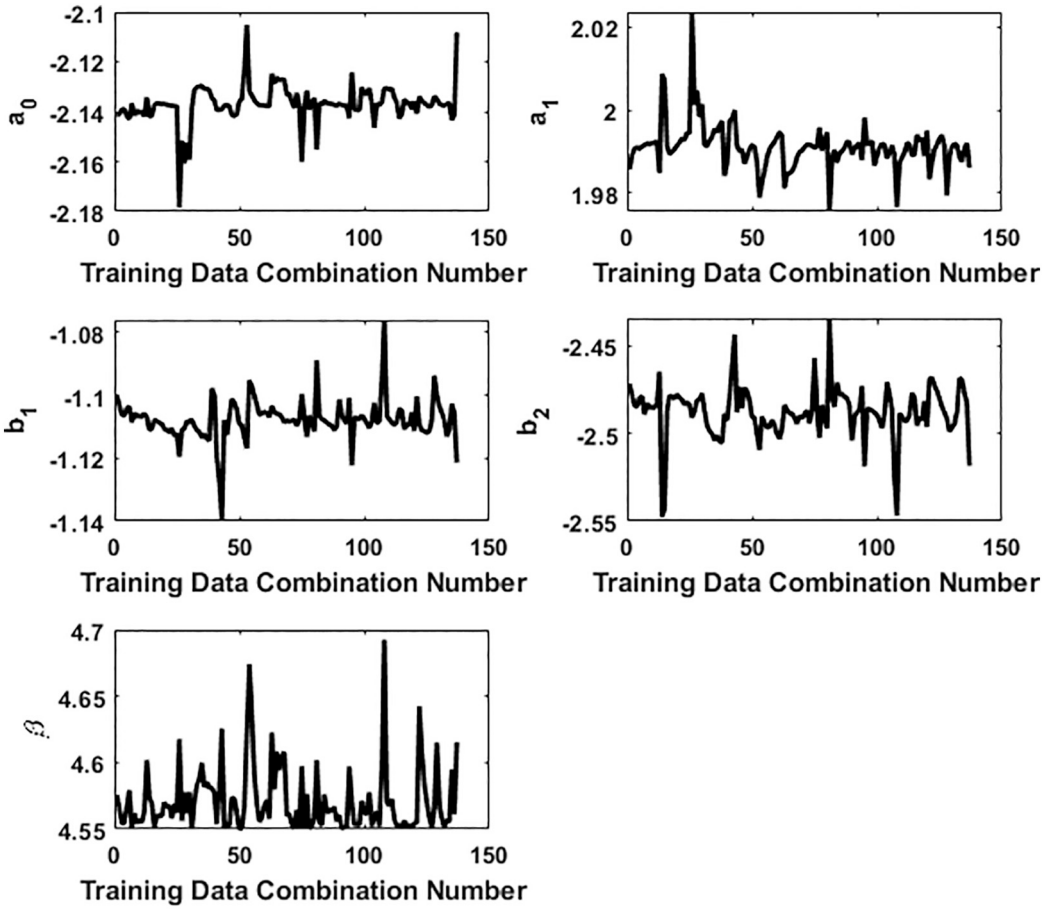

Fig. 14. WAFTR model parameters coefficient variation for different training data combinations.

Data statement

Data associated with this publication are openly available from the NASA prognostics data repository at https://ti.arc.nasa.gov/tech/dash/groups/pcoe/prognostic-data-repository/.

Declaration of competing interest

The authors declare that they have no known competing financial interests or personal relationships that could have appeared to influence the work reported in this paper.

Acknowledgement

The authors gratefully acknowledge the financial support from the UK Engineering and Physical Sciences Research Council (EPSRC, EP/T024844/1 and EP/W004860/1).

References

[1] Liu X, Liu S, Li X, Zhang B, Yue C, Liang SY. Intelligent tool wear monitoring based on parallel residual and stacked bidirectional long short-term memory network. J Manuf Syst 2021;60:608–19. https://doi.org/10.1016/J.JMSY.2021.06.006.
[2] Feng Y, Hung TP, Lu YT, Lin YF, Hsu FC, Lin CF, Lu YC, Liang SY. Flank tool wear prediction of laser-assisted milling. J Manuf Process 2019;43:292–9. https://doi.org/10.1016/J.JMAPRO.2019.05.008.
[3] Wang J, Ma Y, Zhang L, Gao RX, Wu D. Deep learning for smart manufacturing: methods and applications. J Manuf Syst 2018;48:144–56. https://doi.org/10.1016/J.JMSY.2018.01.003.
[4] Yan B, Zhu L, Dun Y. Tool wear monitoring of TC4 titanium alloy milling process based on multi-channel signal and time-dependent properties by using deep learning. J Manuf Syst 2021;61:495–508. https://doi.org/10.1016/J.JMSY.2021.09.017.
[5] Zhou Y, Sun W. Tool Wear condition monitoring in milling process based on current sensors. IEEE Access 2020;8:95491–502. https://doi.org/10.1109/ACCESS.2020.2995586.
[6] Cai W, Zhang W, Hu X, Liu Y. A hybrid information model based on long short-term memory network for tool condition monitoring. J Intell Manuf 2020. https://doi.org/10.1007/s10845-019-01526-4.
[7] Mostaghimi H, Park CI, Kang G, Park SS, Lee DY. Reconstruction of cutting forces through fusion of accelerometer and spindle current signals. J Manuf Process 2021;68:990–1003. https://doi.org/10.1016/J.JMAPRO.2021.06.007.
[8] Zhang J, Starly B, Cai Y, Cohen PH, Lee YS. Particle learning in online tool wear diagnosis and prognosis. JManuf Process 2017;28:457–63. https://doi.org/10.1016/J.JMAPRO.2017.04.012.

[9] Jaen-Cuellar AYosimar, Osornio-Ríos RAlfredo, Trejo-Hernández M, Zamudio-Ramírez I, Díaz-Saldaña G, Pacheco-Guerrero JPablo, Antonino-Daviu JAlfonso, Ragulskis M, Cao M, Zimroz R, Fakher C, Konieczny Ł, Villanueva G. System for tool-wear condition monitoring in CNC machines under variations of cutting parameter based on fusion stray flux-current processing. Sensors 2021;21:8431. https://doi.org/10.3390/S21248431. 21 (2021) 8431.
[10] Kumar A, Parkash C, Vashishtha G, Tang H, Kundu P, Xiang J. State-space modeling and novel entropy-based health indicator for dynamic degradation monitoring of rolling element bearing. Reliab Eng Syst Saf 2022;221:108356. https://doi.org/10.1016/J.RESS.2022.108356.
[11] Proteau A, Tahan A, Thomas M. Specific cutting energy: a physical measurement for representing tool wear. Int J Adv Manuf Technol 2019. https://doi.org/10.1007/s00170-019-03533-4.
[12] Traini E, Bruno G, Lombardi F. Tool condition monitoring framework for predictive maintenance: a case study on milling process. Int J Prod Res 2020. https://doi.org/10.1080/00207543.2020.1836419.
[13] Bagri S, Manwar A, Varghese A, Mujumdar S, Joshi SS. Tool wear and remaining useful life prediction in micro-milling along complex tool paths using neural networks. J Manuf Process 2021;71:679–98. https://doi.org/10.1016/J.JMAPRO.2021.09.055.
[14] Boga C, Koroglu T. Proper estimation of surface roughness using hybrid intelligence based on artificial neural network and genetic algorithm. J Manuf Process 2021;70:560–9. https://doi.org/10.1016/J.JMAPRO.2021.08.062.
[15] Yang WA, Zhou Q, Tsui KL. Differential evolution-based feature selection and parameter optimisation for extreme learning machine in tool wear estimation. Int J Prod Res 2015;54:4703–21. https://doi.org/10.1080/00207543.2015.1111534.
[16] Cheng M, Jiao L, Yan P, Jiang H, Wang R, Qiu T, Wang X. Intelligent tool wear monitoring and multi-step prediction based on deep learning model. J Manuf Syst 2022;62:286–300. https://doi.org/10.1016/J.JMSY.2021.12.002.
[17] Zhu Y, Wu J, Wu J, Liu S. Dimensionality reduce-based for remaining useful life prediction of machining tools with multisensor fusion. Reliab Eng Syst Saf 2022;218:108179. https://doi.org/10.1016/J.RESS.2021.108179.
[18] Lockner Y, Hopmann C, Zhao W. Transfer learning with artificial neural networks between injection molding processes and different polymer materials. J Manuf Process 2022;73:395–408. https://doi.org/10.1016/J.JMAPRO.2021.11.014.
[19] Liao Y, Ragai I, Huang Z, Kerner S. Manufacturing process monitoring using time-frequency representation and transfer learning of deep neural networks. J Manuf Process 2021;68:231–48. https://doi.org/10.1016/J.JMAPRO.2021.05.046.
[20] Han D, Yu J, Tang D. An HDP-HMM based approach for tool wear estimation and tool life prediction. Qual Eng 2021;33:208–20. https://doi.org/10.1080/08982112.2020.1813760/FORMAT/EPUB.
[21] Yu J, Liang S, Tang D, Liu H. A weighted hidden markov model approach for continuous-state tool wear monitoring and tool life prediction. Int J Adv Manuf Technol 2017;91:201–11. https://doi.org/10.1007/S00170-016-9711-0.
[22] Sadhukhan C, Mitra SK, Biswas R, Naskar MK. In: Tool condition monitoring: unscented Kalman filter for tool flank wear estimation in turning of Inconel 718. 25; 2021. p. 331–48. https://doi.org/10.1080/10910344.2020.1855650. doi: 10.1080/10910344.2020.1855650.
[23] Hanachi H, Yu W, Kim IY, Liu J, Mechefske CK. Hybrid data-driven physics-based model fusion framework for tool wear prediction. Int J Adv Manuf Technol 2019;101:2861–72. https://doi.org/10.1007/S00170-018-3157-5.
[24] Li W, Liu T. Time varying and condition adaptive hidden Markov model for tool wear state estimation and remaining useful life prediction in micro-milling. Mech Syst Signal Process 2019;131:689–702. https://doi.org/10.1016/J.YMSSP.2019.06.021.
[25] Kißkalt D, Mayr A, Lutz B, Rögele A, Franke J. Streamlining the development of data-driven industrial applications by automated machine learning. In: Procedia CIRP. Elsevier B.V.; 2020. p. 401–6. https://doi.org/10.1016/j.procir.2020.04.009.
[26] Kundu P, Darpe AK, Kulkarni MS. Gear pitting severity level identification using binary segmentation methodology. Struct Control Health Monit 2020;27(1–20):e2478. https://doi.org/10.1002/stc.2478.
[27] Zhang C, Yao X, Zhang J, Jin H. Tool condition monitoring and remaining useful life prognostic based on awireless sensor in dry milling operations. Sensors (Switzerland) 2016. https://doi.org/10.3390/s16060795.
[28] Cheng C, Li J, Liu Y, Nie M, Wang W. An online belt wear monitoring method for abrasive belt grinding under varying grinding parameters. J Manuf Process 2020;50:80–9. https://doi.org/10.1016/J.JMAPRO.2019.12.034.
[29] Li X, Li HX, Guan XP, Du R. Fuzzy estimation of feed-cutting force from current measurement-a case study on intelligent tool wear condition monitoring. IEEE Trans Syst Man Cybern Part C Appl Rev 2004;34:506–12. https://doi.org/10.1109/TSMCC.2004.829296.
[30] Teti R, Jemielniak K, O'Donnell G, Dornfeld D. Advanced monitoring of machining operations. CIRP Ann 2010;59:717–39. https://doi.org/10.1016/J.CIRP.2010.05.010.
[31] Kumar A, Kumar R. In: Oscillatory behavior-based wavelet decomposition for the monitoring of bearing condition in centrifugal pumps. 232; 2017. p. 757–72. https://doi.org/10.1177/1350650117727976. doi:10.1177/1350650117727976.
[32] Wang J, Liu S, Gao RX, Yan R. Current envelope analysis for defect identification and diagnosis in induction motors. J Manuf Syst 2012;31:380–7. https://doi.org/10.1016/J.JMSY.2012.06.005.
[33] Fu P, Wang J, Zhang X, Zhang L, Gao RX. Dynamic routing-based multimodal neural network for multi-sensory fault diagnosis of induction motor. J Manuf Syst 2020;55:264–72. https://doi.org/10.1016/j.jmsy.2020.04.009.
[34] Kumar A, Tang H, Vashishtha G, Xiang J. Noise subtraction and marginal enhanced square envelope spectrum (MESES) for the identification of bearing defects in centrifugal and axial pump. Mech Syst Signal Process 2022;165:108366. https://doi.org/10.1016/J.YMSSP.2021.108366.
[35] Kumar A, Kumar R. Manifold learning using linear local tangent space alignment (LLTSA) algorithm for noise removal in wavelet filtered vibration signal. J Nondestruct Eval 2016;35:1–10. https://doi.org/10.1007/S10921-016-0366-4/FIGURES/13.
[36] Ebeling CE. An introduction to reliability and maintainability engineering. McGraw-Hill; 2004.
[37] Kundu P, Darpe AK, Kulkarni MS. Weibull accelerated failure time regression model for remaining useful life prediction of bearing working under multiple operating conditions. Mech SystSignal Process 2019;134. https://doi.org/10.1016/j.ymssp.2019.106302.
[38] Kundu P, Chopra S, Lad BK. Multiple failure behaviors identification and remaining useful life prediction of ball bearings. J Intell Manuf 2019;30. https://doi.org/10.1007/s10845-017-1357-8.
[39] Kundu P, Nath T, Palani IA, Lad BK. Integrating GLL-Weibull distribution within a bayesian framework for life prediction of shape memory alloy spring undergoing thermo-mechanical fatigue. J Mater Eng Perform 2018;27:3655–66. https://doi.org/10.1007/s11665-018-3435-2.
[40] Prognostics Center of Excellence. Data repository. https://ti.arc.nasa.gov/tech/dash/groups/pcoe/prognostic-data-repository/. [Accessed 20 August 2020].
[41] Kundu P, Darpe AK, Kulkarni MS. A review on diagnostic and prognostic approaches for gears. Struct Health Monit 2020:1–41. https://doi.org/10.1177/1475921720972926.